Electronic Supplementary Information

Multiscale structures and rheology of bisurea-loaded resins for anti-sagging application

Ying-Feng He,[†] Ssu-Ting Huang,[†] Chia-Hao Chen,[†] Yu-Hsuan Chang,[†] Chi-Chung Hua,*[†] Ping-Ray Chiang,*[‡] Jien-Yi Weng,[‡]

[†]*Department of Chemical Engineering, National Chung Cheng University, Chia-Yi 621301, Taiwan*

[‡]*Fundamental Research Technical Team of R&D Division, Eternal Materials Co., Ltd., Kaohsiung 821010, Taiwan*

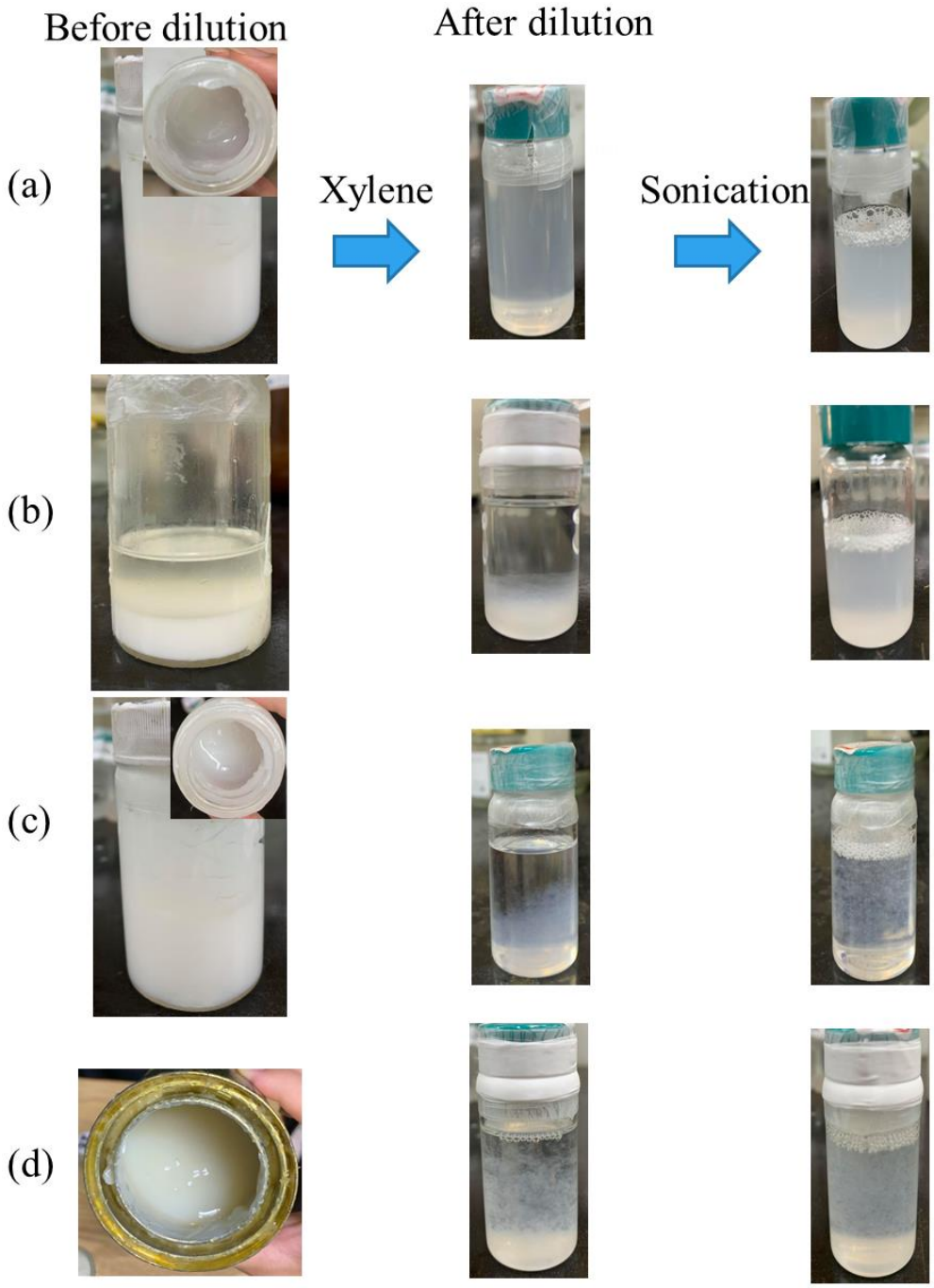

Fig. S1 Photographs showing the appearance of four BLRs before and after dilution: (a) HDI-BA, (b) IPDI-BA, (c) MDI-BA, and (d) TDI-BA resins. The dilute samples were used mainly for DLS and SALS analyses.

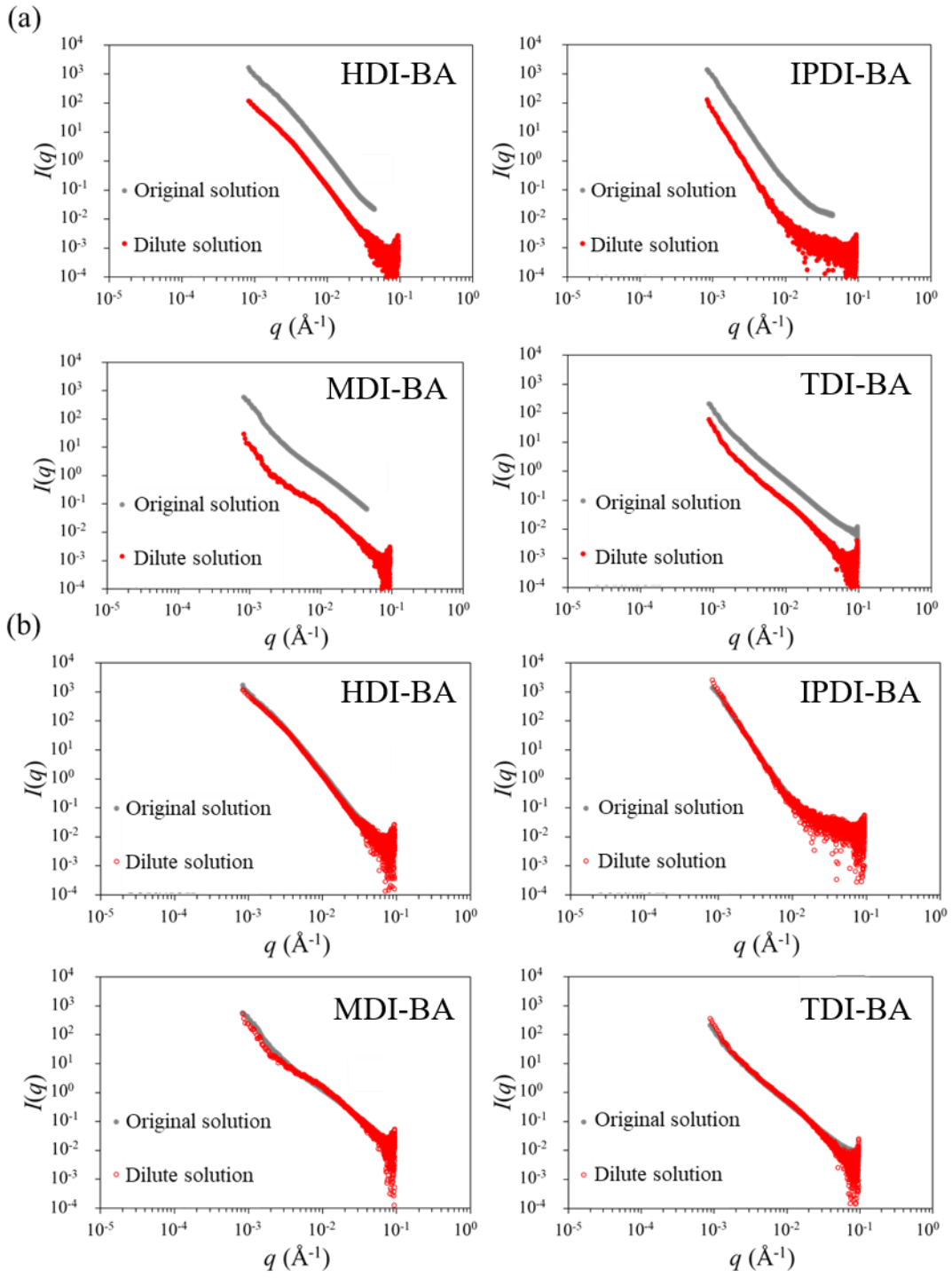

Fig. S2 (a) Comparison of SAXS data between the original and dilute BLRs at $T = 25$ °C. (b) Overlap of the SAXS data after arbitrary vertical shifts for the dilute samples.

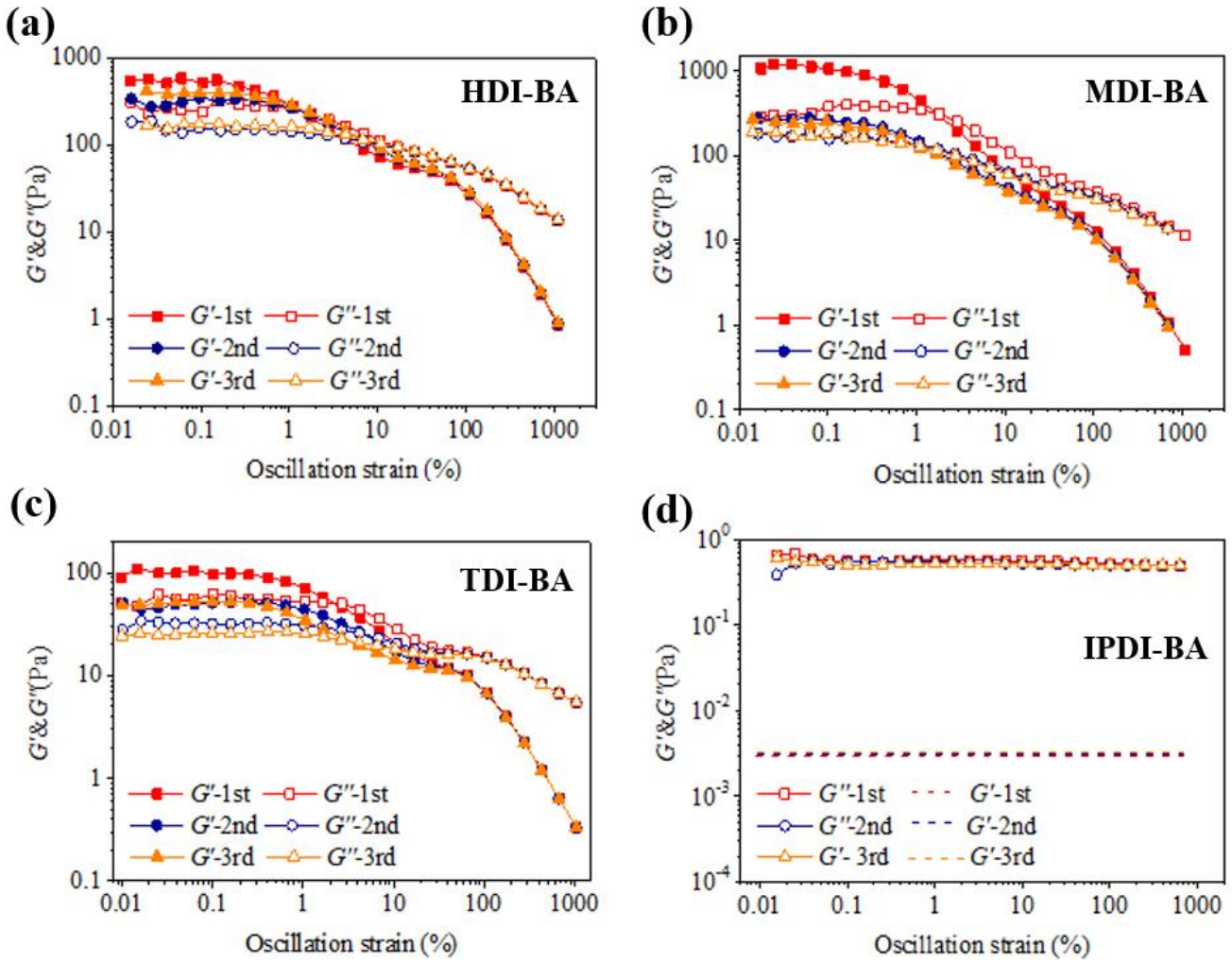

Fig. S3 Results on pre-shearing treatment using repeated strain sweeps at a frequency of 1.0 Hz for (a) HDI-BA, (b) MDI-BA, (c) TDI-BA, and (d) IPDI-BA resins.

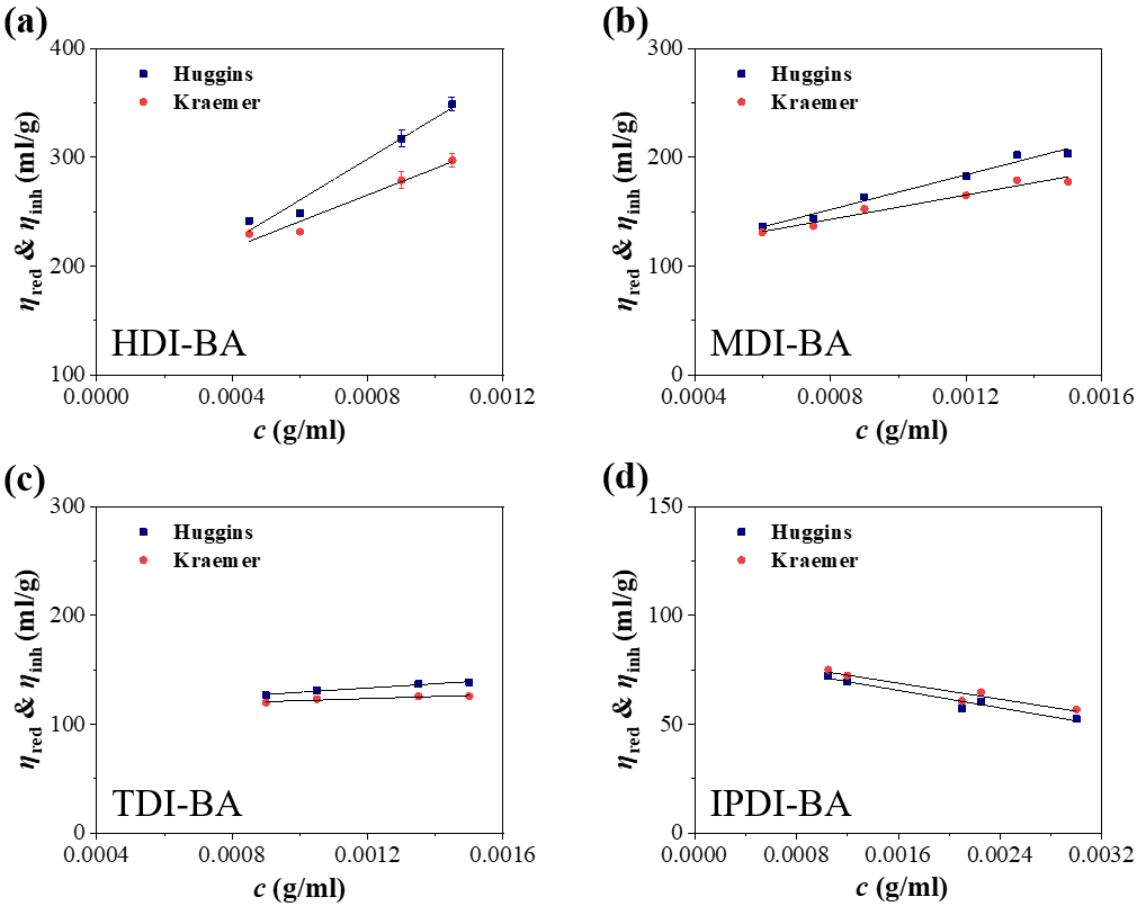

Fig. S4 Original viscosity data along with two different extrapolation schemes used to determine the intrinsic viscosity on (a) HDI-BA, (b) MDI-BA, (c) TDI-BA, and (d) IPDI-BA resins at $T = 25.0$ ℃.

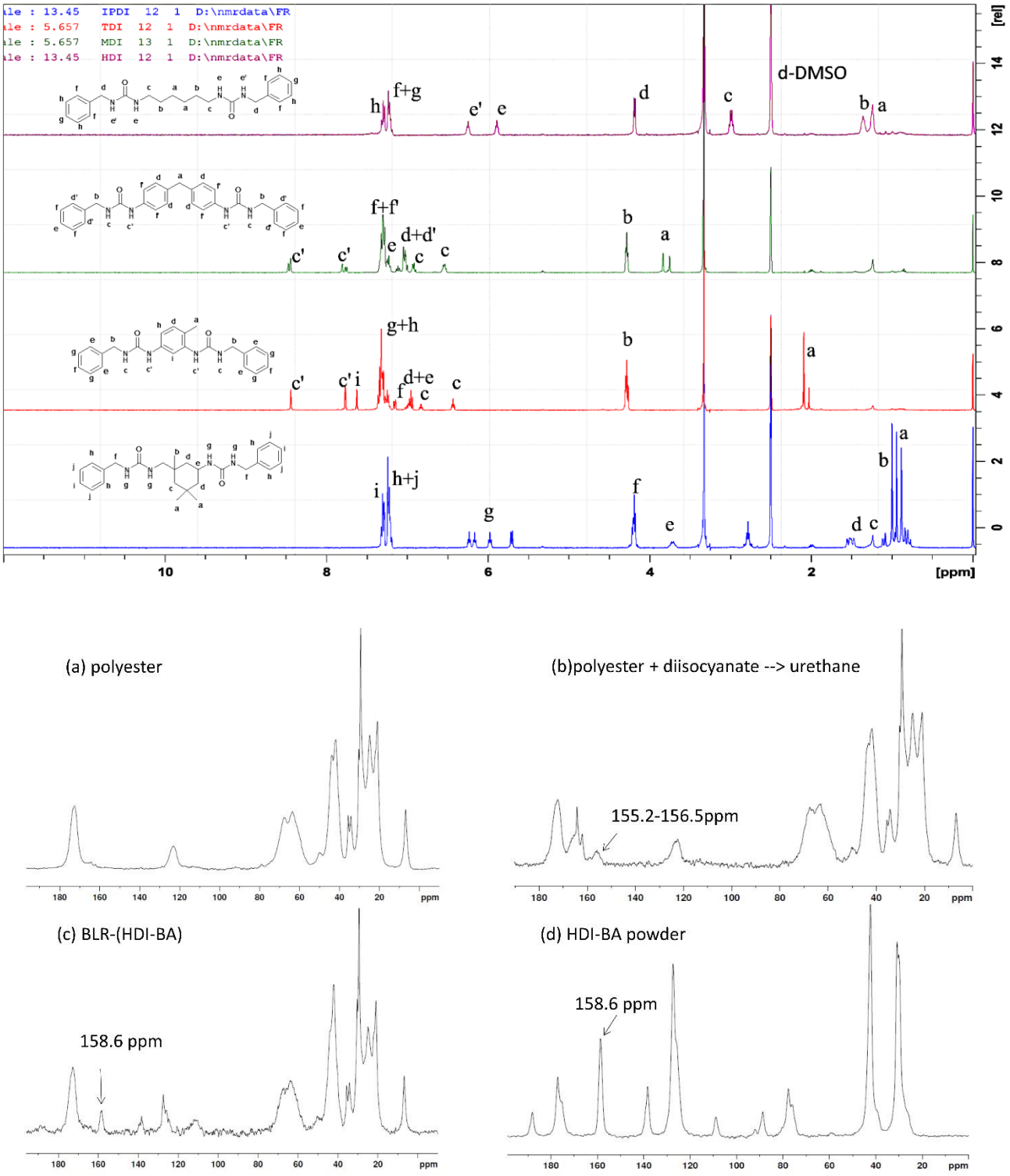

Fig. S5 (Top) ^{1}H NMR spectra of HDI-BA, MDI-BA, TDI-BA, and IPDI-BA aggregates isolated from the respective BLRs in d-DMSO. The MDI consists of 2,4-MDI (55 wt.%) and 4,4-MDI (45 wt.%) two different isomers, and therefore the MDI-BA represents a mixture and the spectrum is asymmetric.

(Bottom) Comparison of ^{1}H solid-NMR spectra for four different samples. The peak at 155.2-156.5 ppm in (b) indicates the formation of urethane by the reaction of polyester and HDI at a temperature of T = 60 °C, while (c) the BLR (HDI-BA) dried at 150 °C for 15 min to remove the solvent *ortho*-xylene and (d) the HDI-BA powder (see the preparatory scheme in Fig. S7) reveal no such peak and, instead, share a common peak at 158.6 ppm for urea. The results are consistent with the DSC characterization in Fig. S6, indicating the formation of urethane for the polyester and HDI mixing system at temperatures above T = 11 °C. Note that the peak at 120 ppm in (a) denotes the benzene ring structure of residual *ortho*-xylene, and the peaks at 75 and 190 ppm in (d) are contributed by unknown side products during the preparation of the bisurea powder.

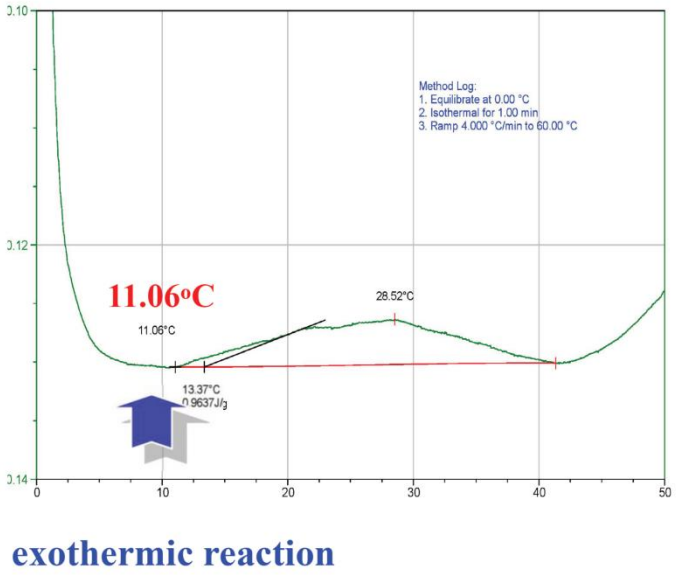

Fig. S6 DSC characterization of the polyester and HDI mixing system at a weight ratio of 1:0.1. The result reveals an exothermic reaction and formation of urethane at temperatures above T = 11 °C.

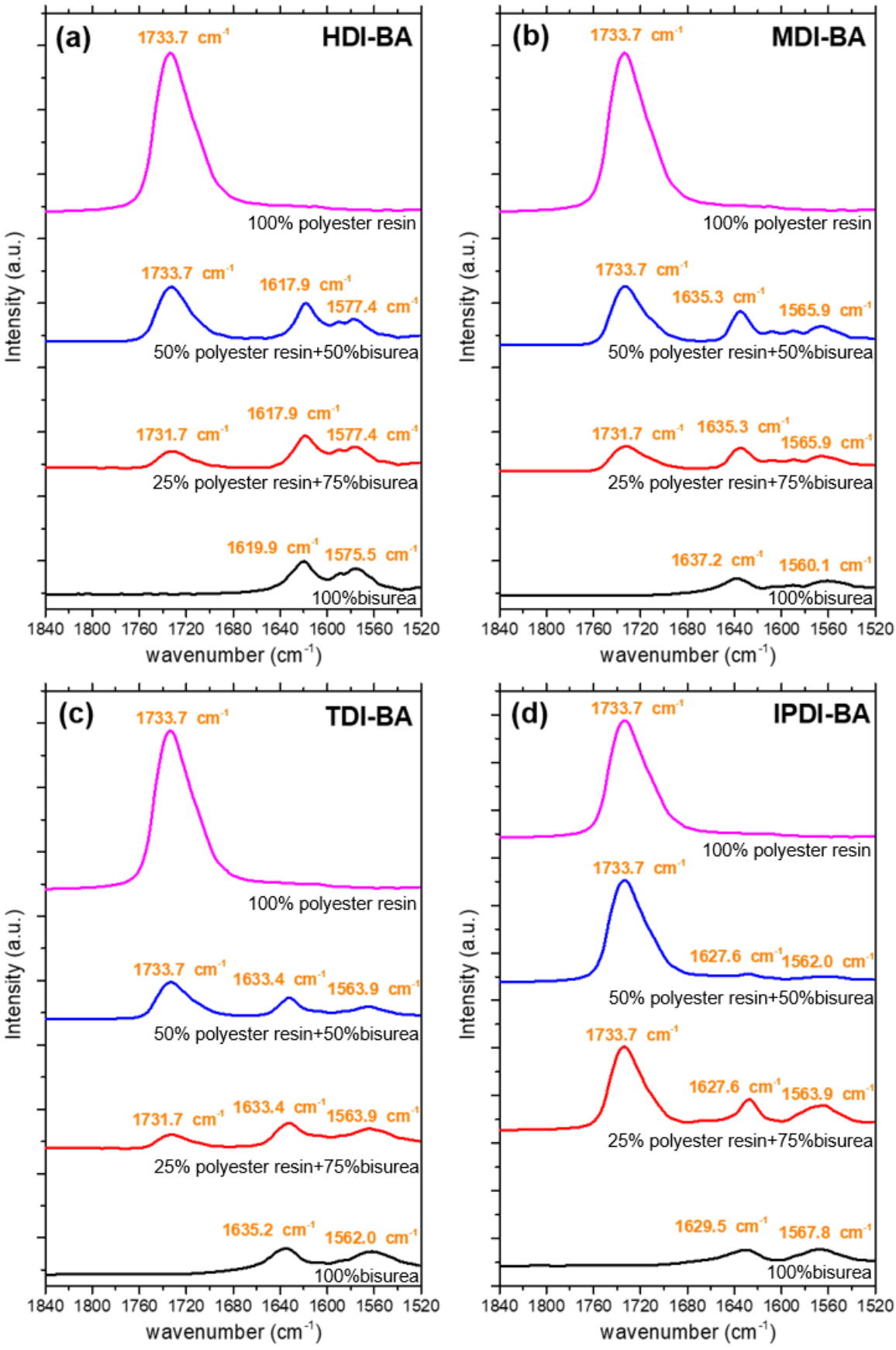
(a)
HDI-BA
1733.7 cm-1
100% polyester resin
1733.7 cm-1
1617.9 cm-1
1577.4 cm-1
50% polyester resin+50%bisurea
1731.7 cm-1
1617.9 cm-1
1577.4 cm-1
25% polyester resin+75%bisurea
1619.9 cm-1
1575.5 cm-1
100%bisurea
(b)
MDI-BA
1733.7 cm-1
100% polyester resin
1733.7 cm-1
1635.3 cm-1
1565.9 cm-1
50% polyester resin+50%bisurea
1731.7 cm-1
1635.3 cm-1
1565.9 cm-1
25% polyester resin+75%bisurea
1637.2 cm-1
1560.1 cm-1
100%bisurea
(c)
TDI-BA
1733.7 cm-1
100% polyester resin
1733.7 cm-1
1633.4 cm-1
1563.9 cm-1
50% polyester resin+50%bisurea
1731.7 cm-1
1633.4 cm-1
1563.9 cm-1
25% polyester resin+75%bisurea
1635.2 cm-1
1562.0 cm-1
100%bisurea
(d)
IPDI-BA
1733.7 cm-1
100% polyester resin
1733.7 cm-1
1627.6 cm-1
1562.0 cm-1
50% polyester resin+50%bisurea
1733.7 cm-1
1627.6 cm-1
1563.9 cm-1
25% polyester resin+75%bisurea
1629.5 cm-1
1567.8 cm-1
100%bisurea
Intensity (a.u.)
1840 1800 1760 1720 1680 1640 1600 1560 1520
wavenumber (cm-1)

Fig. S7 Comparison of FTIR spectra for the polyester resin/bisurea powder mixtures at various weight ratios for (a) HDI-BA, (b) MDI-BA, (c) TDI-BA, and (d) IPDI-BA as the bisurea. The bisurea used here was synthesized in an organic solvent, *ortho*-xylene, at room temperature using benzylamine (BA) and four different types of diisocyanates. The product was then precipitated and purified in the final form of powder. The powder was later blended with the polyester resin at room temperature and two different weight ratios to investigate the physical interactions between polyester and bisurea molecules through FTIR spectroscopy analysis. The excess amount of bisurea used in the blends, compared with the composition of BLRs, was aimed to enhance the FTIR signals for the above-mentioned purpose. The results indicate that, except for the polyester-IPDI-BA mixture, there is a clear shift from 1733.7 to 1731.7 cm^{-1} for the vibration band of C=O groups of polyester for the 25/75 blends (polyester/bisurea/*ortho*-xylene = 18.75/75/6.25 wt.%), attributable to the formation of hydrogen bond between polyester and bisurea. The reason that the 50/50 blends (polyester/bisurea/*ortho*-xylene = 37.5/50/12.5 wt.%) show no such shift might be ascribed to the fact that only a very small amount of polyester participating in the hydrogen bonding with bisurea, so that the remaining non-bonded polyester would dominate the main absorption peak at 1733.7 cm^{-1}.

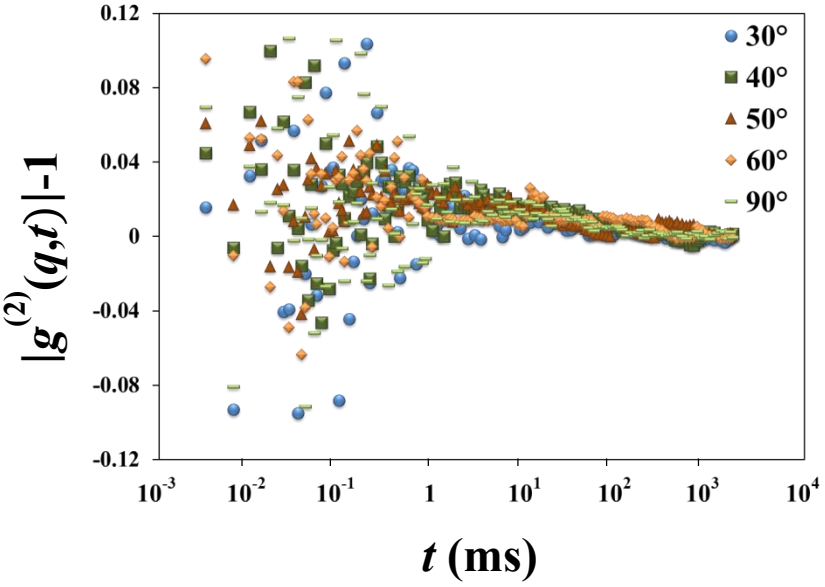

Fig. S8 Original DLS data on the 49 wt.% polyester/*ortho*-xylene solution. The result shows no discernible relaxation pattern, indicative of little or no aggregation of polyester molecules.

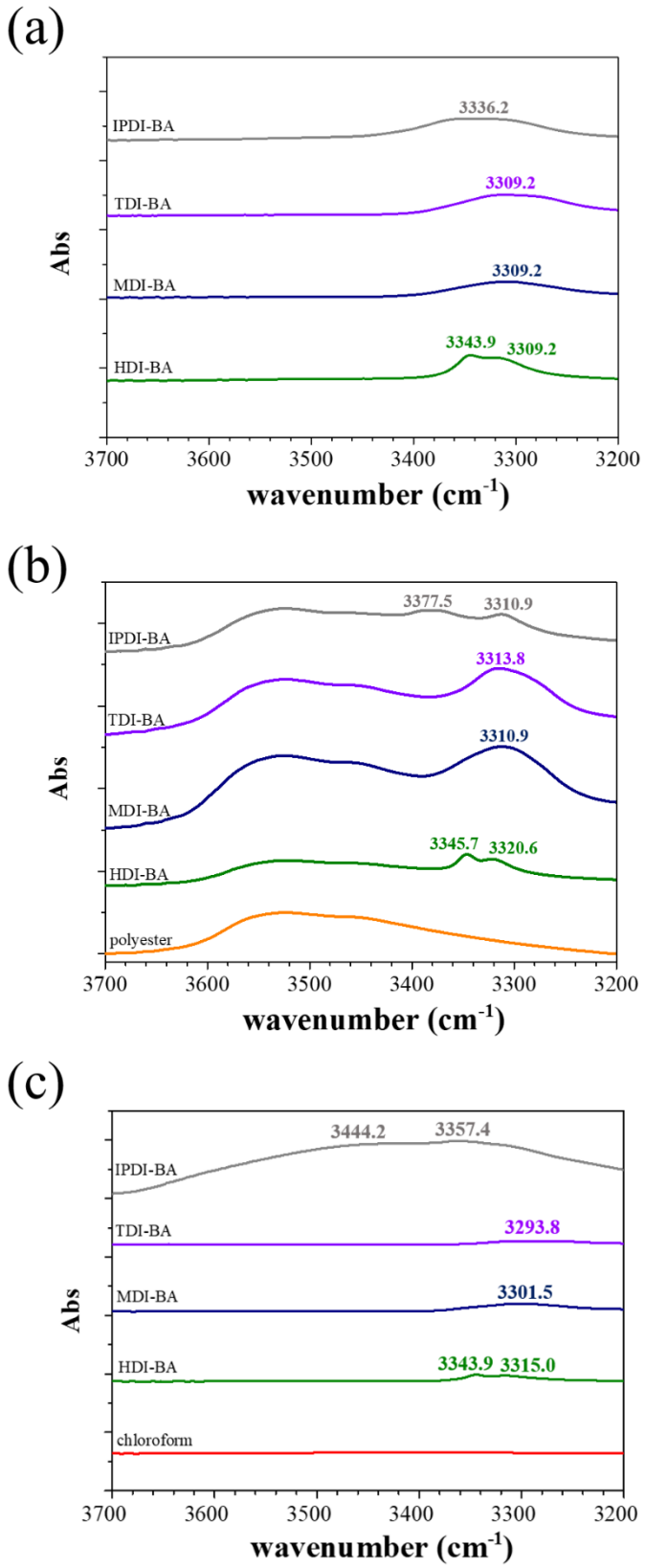

Fig. S9 Comparison of FTIR spectra for (a) bisurea powder, (b) BLR, and (c) bisurea/chloroform (30 mg mL^{-1}) samples.

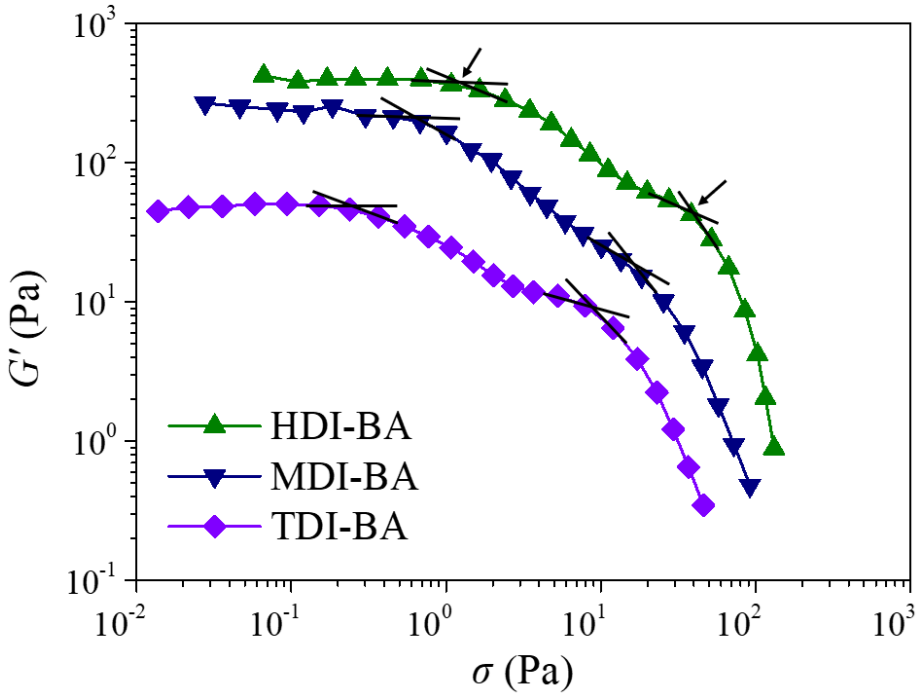

Fig. S10 Storage modulus as a function of the stress amplitude during strain sweep at 1.0 Hz and 25.0 ℃ for three BLRs that exhibit two distinct yield points.

S1 Determination of volume fraction

The following equation for dilute colloidal suspensions[1] is used to determine the volume fraction, ϕ, of a dilute BLR sample:

$$\frac{\eta}{\eta_0} = 1 + k_1\phi \quad \text{(S1)}$$

where η denotes the solution viscosity at a given concentration, η_0 is the medium viscosity (=0.68 cp), and $k_1 = [\eta]$.

S2 Model fits of SALS/SAXS data:

The SALS data in Fig. 3 on each of the BLRs can be used to determine the mean radius of gyration, R_g, of the agglomerate species as well as to capture its mass-fractal structure using the following formulation:[2]

$$I_{\text{agglomerate}}(q) = G \exp\left(\frac{-q^2 {R_g}^2}{3}\right) \text{, for } q \le q_1 \tag{S2}$$

$$I_{\text{agglomerate}}(q) = \frac{B}{q^{D_m}} \text{ , for } q \ge q_1$$

$$q_1 = \frac{1}{R_g}\left(\frac{3D_m}{2}\right)^{1/2}$$

where G and B are two scale factors, and D_m denotes the mass-fractal exponent.

The low-q SAXS data can be used to resolve the detailed interior structure of an agglomerate species. For the HDI-BA, MDI-BA, and TDI-BA resins, by treating the constituting helical rods as cylinders, whose form factor requires fewer parameters than that for helical rods,[3] the following combination of form and structure factors can be utilized to capture the SAXS data in this region:

$$I_{\text{agglomerate}}(q) = k\, S(q)\, P_{\text{cylinder}}(q) \tag{S3}$$

$$P_{\text{cylinder}}(q) = \int_0^{\pi/2} \left[\frac{\sin(\frac{1}{2}qL\cos\phi)}{\frac{1}{2}qL\cos\phi} \frac{2J_1(qR\sin\phi)}{qR\sin\phi}\right] \tag{S4}$$

where k is a scale factor, L and R (=1/2 D_r in Table 1) denote the length and radius of the cylinder, respectively, and ϕ is the angle between the long axis of the cylinder and the primary beam.[4,5] Thus, eqn (S4) describes the form factor of randomly packed cylinders, consistent with the structure factor

used in eqn (S3).

As discussed in the main text, two different structure factors are required in eqn (S3). For the HDI-BA resin, the cylindrical aggregates form loosely packed, mesh-like network structure. Therefore, the following formula previously employed to describe a mesh network of cylinders[6] is used:

$$S(q) = \frac{I_L(0)}{\{1+[(d_f+1)/3]\zeta^2 q^2\}^{d_f/2}} \tag{S5}$$

where d_f and ζ denote the mass-fractal exponent and mesh size, respectively.

For the MDI-BA and TDI-BA resins, a general expression for describing the mass-fractal network structure[4,7] is found to be sufficient because the cylindrical aggregates form a compact network structure:

$$S(q) = 1 + \frac{D_m\,\Gamma(D_m-1)\sin[(D_m-1)\tan^{-1}(q\zeta)]}{(qr_0)^{D_m}\,(1+1/(q\zeta)^2)^{(D_m-1)/2}} \tag{S6}$$

where D_m has a similar meaning as d_f in eqn (S5), ζ here represents the cut-off distance beyond which the mass-fractal structure ceases to apply, and r_0 denotes the dimension of the constituting objects. To distinguish between the mass-fractal exponents determined from the SALS and SAXS data, respectively, the value of D_m fitted from the SAXS data is denoted as d_f in Table 1.

For the high-q SAXS data, there is a second Guinier region which marks the form factor of the elementary packing unit. For the cases with HDI-BA, MDI-BA, and TDI-BA resins, eqn (S4) can be used to describe the rod-like feature of the packing unit. The rod length and diameter are denoted as l

and d_r in Table 1.

The SAXS intensity profiles for the IPDI-BA resin differ notably from those for the other BLRs. While the data in the low-q region reveal a surface-fractal structure[8] instead, the data in the high-q region can be well described by the form factor of spherical packing units. Accordingly, the following expressions are employed:

$$I_{\text{agglomerate}}(q) = k\, S(q)\, P_{\text{sphere}}(q) \tag{S7}$$

$$S(q) = 1 + \frac{9\phi_b \Gamma(5-D_s)}{(2qr_0)^{6-D_s}} \frac{\sin[\pi(3-D_s)/2]}{3-D_s} \tag{S8}$$

$$P_{\text{sphere}}(q) = \left[3\frac{\sin(qR) - qR\cos(qR)}{qR^3}\right]^2 \tag{S9}$$

where D_s represents the surface-fractal exponent and, for consistency, is denoted as d_f in Table 1, ϕ_b represents the fraction of building (intermediate) aggregate species located at the fractal surface boundary, and r_0 denotes the dimension of an aggregate. In the above formulation, the aggregate species which constitutes the network structure is assumed to be sphere-like, with the diameter denoted as D_s in Table 1. For the high-q SAXS data, the same formula as with eqn (S9) is used to describe the form factor of the spherical packing unit, whose diameter is denoted as d_s in Table 1.

References

1. L. Jowkarderis and T. G. van de Ven, *Cellulose*, 2014, **21**, 2511-2517.
2. B. Hammouda, *J. Appl. Crystallogr.*, 2010, **43**, 716-719.
3. C. L. Pizzey, W. C. Pomerantz, B.-J. Sung, V. M. Yuwono, S. H. Gellman, J. D. Hartgerink, A. Yethiraj and N. L. Abbott, *J. Chem. Phys.*, 2008, **129**, 09B603.
4. R. H. Guo, C. C. Hua, P. C. Lin, T. Y. Wang and S. A. Chen, *Soft Matter*, 2016, **12**, 6300-6311.
5. T. M. Stawski, R. Besselink, S. A. Veldhuis, H. L. Castricum, D. H. Blank and J. E. ten Elshof, *J. Colloid Interface Sci.*, 2012, **369**, 184-192.
6. H. L. Yi and C. C. Hua, *Soft Matter*, 2019, **15**, 8022-8031.
7. J. Teixeira, *J. Appl. Crystallogr.*, 1988, **21**, 781-785.
8. R. Besselink, T. M. Stawski, A. E. S. Van Driessche and L. G. Benning, *J. Chem. Phys.*, 2016, **145**, 211908.